

**Planets in Stellar Clusters Extensive Search. V. Search for planets and identification of 18 new variable stars in the old open cluster NGC 188.<sup>1</sup>**

**Mochejska, B. J.,**

Copernicus Astronomical Center, ul. Bartycka 18, 00-716 Warszawa, Poland  
e-mail: mochejsk@camk.edu.pl

**Stanek, K. Z.,**

Department of Astronomy, The Ohio State University, 140 W. 18th Avenue, Columbus,  
OH 43210, USA  
e-mail: kstanek@astronomy.ohio-state.edu

**Sasselov, D. D., Szentgyorgyi, A. H., Cooper, R. L., Hickox, R. C.,  
Hradecky, V.**

Harvard-Smithsonian Center for Astrophysics, 60 Garden St., Cambridge, MA 02138,  
USA  
e-mail: sasselov, saint, rcooper, rhickox, vhradecky@cfa.harvard.edu

**Marrone, D. P.**

Jansky Postdoctoral Fellow, National Radio Astronomy Observatory; Kavli Institute for  
Cosmological Physics, University of Chicago, 5640 South Ellis Avenue, Chicago, IL,  
60637, USA  
e-mail: dmarrone@uchicago.edu

**Winn, J. N.**

Department of Physics, and Kavli Institute for Astrophysics and Space Research,  
Massachusetts Institute of Technology, Cambridge, MA, USA  
e-mail: jwinn@cfa.harvard.edu

**Schwarzenberg-Czerny, A.**

Astronomical Observatory of Adam Mickiewicz University, ul. Słoneczna 36, 60-286  
Poznan, Poland; Copernicus Astronomical Center, ul. Bartycka 18, 00-716 Warszawa,

---

<sup>1</sup>Based on data from the FLWO 1.2m telescope

Poland  
e-mail: alex@camk.edu.pl

*Received Month Day, Year*

## ABSTRACT

We have undertaken a long-term project, Planets in Stellar Clusters Extensive Search (PISCES), to search for transiting planets in open clusters. In this paper we present the results for NGC 188, an old, rather populous cluster. We have monitored the cluster for more than 87 hours, spread over 45 nights. We have not detected any good transiting planet candidates. We have discovered 18 new variable stars in the cluster, bringing the total number of identified variables to 46, and present for them high precision light curves, spanning 15 months.

**Key words:** *planetary systems – binaries: eclipsing – cataclysmic variables – stars: variables: other – color-magnitude diagrams*

## 1. Introduction

We have undertaken a long-term project, Planets in Stellar Clusters Extensive Search (PISCES), to search for transiting planets in open clusters. To date we have published a feasibility study based on one season of data for NGC 6791 (Mochejska et al. 2002, hereafter Paper I) and a catalog of 57 variable stars for our second target, NGC 2158, based on the data from the first observing season (Mochejska et al. 2004, hereafter Paper II). We have also published the results of an extensive search for transiting planets in NGC 6791, based on over 300 hours of observations, spread over 84 nights (Mochejska et al. 2005, hereafter Paper III). We have not detected any promising candidates, and derived an estimate of 1.5 expected transiting planets. Our search in NGC 2158 (Mochejska et al. 2006, hereafter Paper IV) produced a candidate transiting low-luminosity object with eclipse depth of 3.7% in the  $R$  band.

In this final paper of the series we present the results of a search for transiting planets and variable stars in the open cluster NGC 188  $[(\alpha, \delta)_{2000} = (0^h 48^m, +85^\circ 15'); (l, b) = (122^\circ .86, +22^\circ .38)]$ . It is a rather populous, old ( $\tau = 7$  Gyr), solar metallicity ( $[Fe/H] = -0.04$ ) cluster, located at a distance modulus of  $(m - M)_V = 11.44$  (von Hippel & Sarajedini 1998; Sarajedini et al. 1999).

The paper is arranged as follows: §2 describes the observations, §3 summarizes the reduction procedure, §4 outlines the search strategy for transiting planets, §5 gives an estimate of the expected number of transiting planet detections and §6 contains the variable star catalog. Concluding remarks are found in §7.

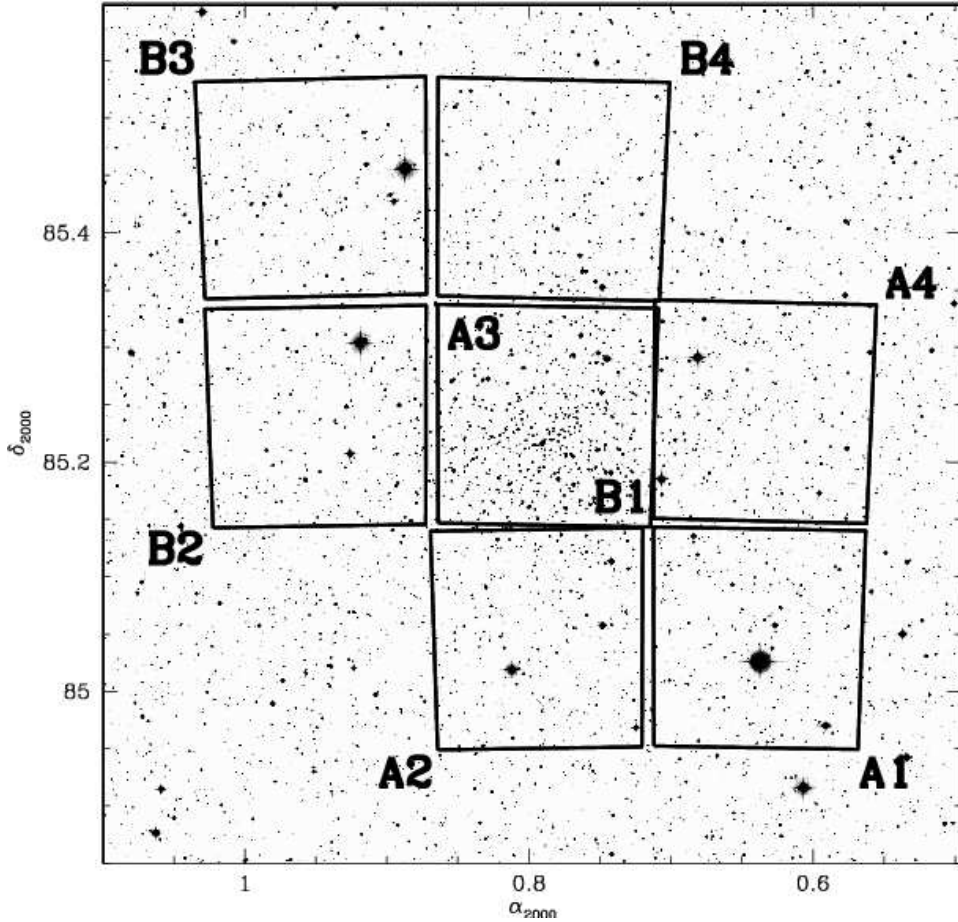


Fig. 1. Digital Sky Survey image of NGC 188 showing fields A and B. The chips in each field are numbered clockwise from 1 to 4 starting from the bottom right chip. NGC 188 is centered on chips A3 and B1. North is up and east is to the left.

## 2. Observations

The data analyzed in this paper were obtained at the Fred Lawrence Whipple Observatory (FLWO) 1.2 m telescope using the 4Shooter CCD mosaic with four thinned, back side illuminated AR coated Loral 2048<sup>2</sup> CCDs (Szentgyorgyi et al. in preparation). The camera, with a scale of 0''.33 pixel<sup>-1</sup>, gives a field of view of 11'.4 × 11'.4 for each chip. Two fields, A and B, were monitored, with the cluster centered on chip 3 in field A and chip 1 in field B (Fig. 1). The data were collected during 45 nights, from 2002 September 9 to 2003 December 17. We obtained a total of 840 × 300 s exposures in the *R*-band (474 for field A and 366 for B) and 208 × 300 s exposures in the *V*-band (118 for field A and 80 for B).

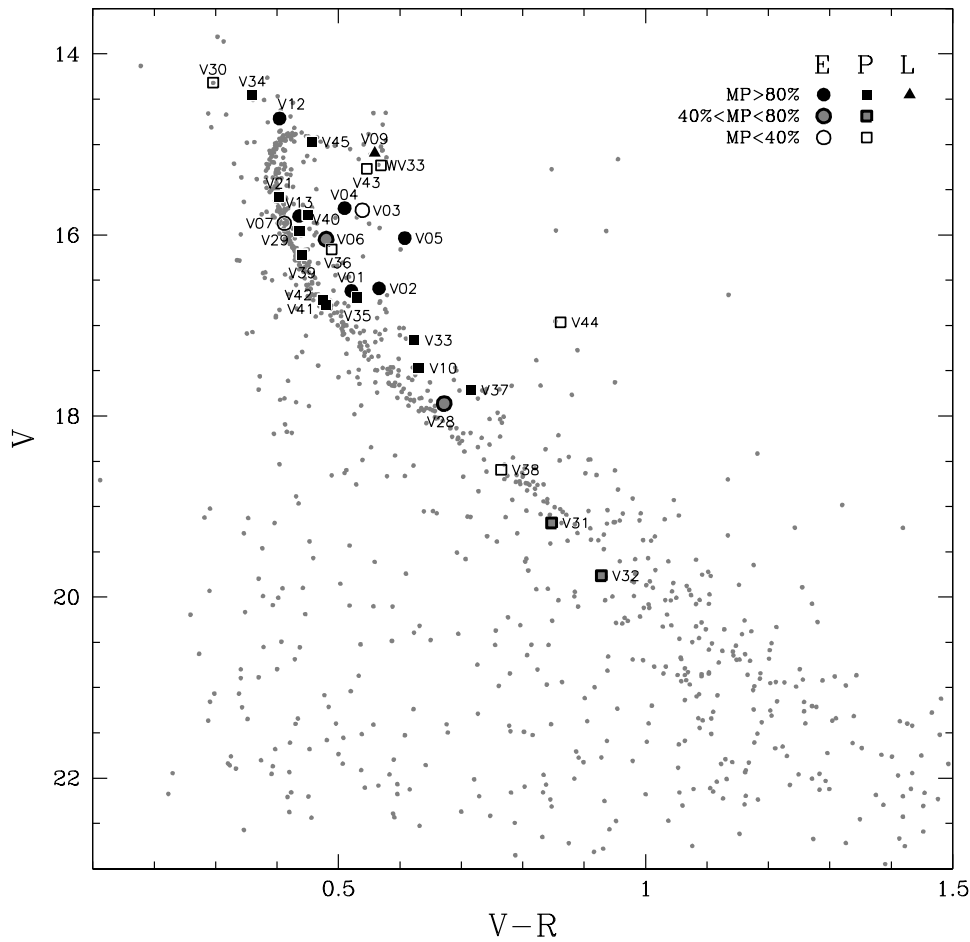


Fig. 2.  $V/V-R$  CMD for chip A3, centered on NGC 188. Eclipsing binaries are plotted with circles, other periodic variables with squares and the non-periodic variable with a triangle. Filled symbols indicate membership probability  $MP > 80\%$ , gray symbols  $40\% < MP < 80\%$  and open symbols  $MP > 40\%$ .

### 3. Data Reduction

#### 3.1. Image Subtraction Photometry

The preliminary processing of the CCD frames was performed with the standard routines in the IRAF ccdproc package.<sup>2</sup>

Photometry was extracted using the ISIS image subtraction package (Alard & Lupton 1998; Alard 2000), as described in detail in Papers I and III.

The ISIS reduction procedure consists of the following steps: (1) transformation of all frames to a common  $(x,y)$  coordinate grid; (2) construction of a refer-

<sup>2</sup>IRAF is distributed by the National Optical Astronomy Observatories, which are operated by the Association of Universities for Research in Astronomy, Inc., under cooperative agreement with the NSF.

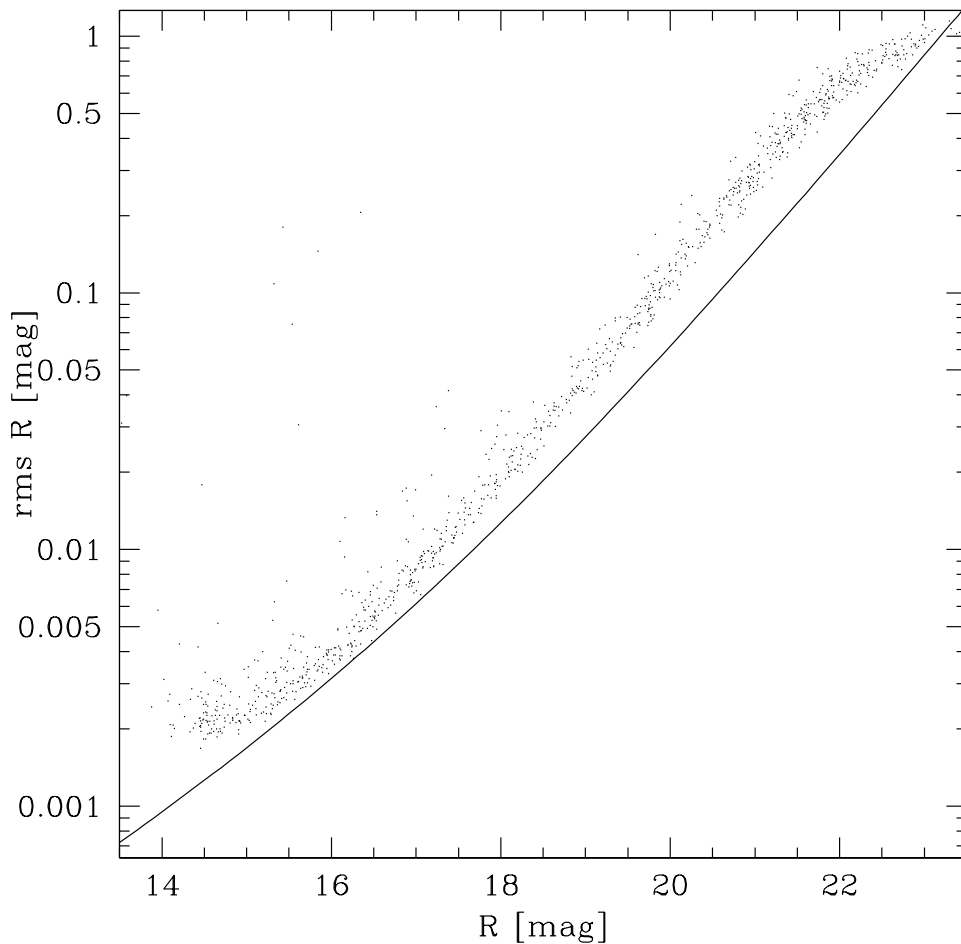


Fig. 3. The rms scatter of the  $R$ -band light curves for stars on chip 3, field A, with at least 200 data points. The solid curve indicates the photometric precision limit due to Poisson noise of the star and average sky brightness.

ence image from several of the best exposures; (3) subtraction of each frame from the reference image; (4) selection of stars to be photometered and (5) extraction of profile photometry from the subtracted images.

We used the same parameters for image subtraction as in Paper III. The reference images were constructed from 20 best exposures in  $R$  and 15 in  $V$ .

### 3.2. Calibration

The  $VR$  photometry was calibrated against the catalog of Stetson et al. (2004). The zero points in the  $R$ -band were derived from 44, 99, 547 and 149 stars in chips A1-A4 and 522, 101, 54 and 133 stars in chips B1-B4. The zero points in the  $V$ -band were derived from 206, 247, 514 and 281 stars in chips A1-A4 and 495, 251, 222 and 261 stars in chips B1-B4. The rms scatter of the residuals was 0.02-0.03 in  $R$  on chips with at least 100 stars, and 0.04-0.06 on the remaining

three chips, and 0.02-0.04 in  $V$  on all chips.

Figure 2 shows the calibrated  $V/V-R$  color-magnitude diagram (CMD) for the chip A3 reference image.

### 3.3. Astrometry

Equatorial coordinates were determined for the  $R$ -band reference image star lists. The transformation from rectangular to equatorial coordinates was derived using 149, 182, 518 and 212 transformation stars in chips A1-A4, and 506, 190, 161 and 199 stars in chips B1-B4, respectively, from the 2MASS catalog (Cutri et al. 2003). The rms deviation between the catalog and the computed coordinates for the transformation stars was  $1''.0 - 1''.3$  in right ascension (quite large, due to the closeness of the cluster to the north celestial pole) and  $0''.1$  in declination.

## 4. Search for Transiting Planets

### 4.1. Further Data Processing

We rejected from further analysis 59 field A and 63 field B  $R$ -band epochs where the full-width at half-maximum (FWHM) of the stellar point-spread function (PSF) was greater than 10 pixels and fewer than 1000 stars were detected on chips 3A and 1B by DAOPhot (Stetson 1987). We also rejected additional 53 field A and 34 field B bad quality images. This left us with 362 and 269 highest quality  $R$ -band exposures in fields A and B, with a median seeing of  $2''.2$ . We also removed 4 and 5  $V$ -band images from fields A and B, which left us with 114 and 85 exposures with a median seeing of  $2''.6$ .

Correcting the light curves for systematic effects using the Tamuz et al. (2005) method alone was insufficient, based on the results of simulations identical to those described in §5.2. We found significant improvement in the results of the simulations when we also corrected the data for the presence of offsets between the observing runs. These offsets are probably caused by the periodic UV flooding of the CCD camera, which alters its quantum efficiency as a function of wavelength. Following the procedure used in Paper III, the light curves were corrected by adding offsets to different runs, individually for each light curve, so that the median magnitude was the same during each run. There were four runs, each spanning from 59 to 167 points in field A and 42 to 126 points in field B. Typical sizes of the offsets on chips A3 and B1 were, respectively, 0.001 and 0.002 for stars below  $R=18$  and 0.008 and 0.009 for stars between  $R=18$  and 19.

Fig. 3 shows the rms scatter of the  $R$ -band light curves for stars on chip A3 with at least 200 data points. The solid curve indicates the photometric precision limit due to Poisson noise of the star and average sky brightness.

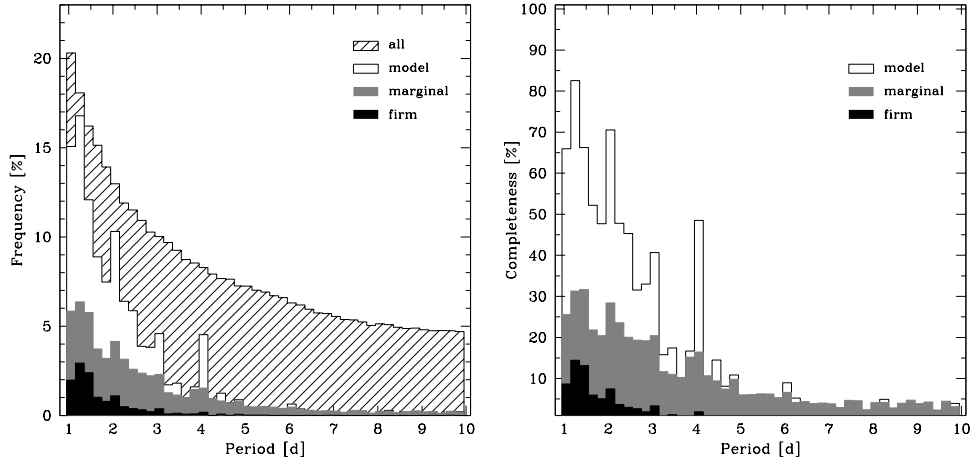


Fig. 4. Detection efficiency of transiting planets as a function of their period, relative to planets with all inclinations (*left*) and all transiting planets (*right*). Shown are the distributions for all transiting planets (*hatched histogram*), detections in the model light curves (*open histogram*) and marginal (*filled gray histogram*) and firm (*filled black histogram*) detections in the combined light curves.

#### 4.2. Selection of Transiting Planet Candidates

For further analysis we selected stars with at least 200 good epochs, magnitudes  $R > 14.88$  (the main sequence turnoff; MSTO) and light curve rms below 0.05 mag. This left us with 2031 stars: 171, 201, 461 and 232 on chips A1-A4 and 371, 208, 192 and 195 on chips B1-B4.

To select transiting planet candidates we used the box-fitting least-squares (BLS) method (Kovács, Zucker, & Mazeh 2002). Adopting a cutoff of 5 in Signal Detection Efficiency (SDE) and 9 in effective signal-to-noise ratio ( $\alpha$ ), we selected 25 stars on all chips. Among these we did not find any good transiting planet candidates.

### 5. Estimate of the Number of Expected Detections

To allow for a direct comparison with our previous transiting planet searches in NGC 6791 (Paper III) and NGC 2158 (Paper IV), we have used the same method and parameters to estimate the number of expected detections. We derived the number of transiting planets we should expect to find,  $N_P$ , from the following equation:

$$N_P = N_* f_P D \quad (1)$$

where  $N_*$  is the number of stars with sufficient photometric precision,  $f_P$  is the frequency of planets within the investigated period range and  $D$  is the detection efficiency, which accounts for random inclinations. ( $N_*$ ). In §§5.1 and 5.2 we determine  $f_P$  and  $D$ .

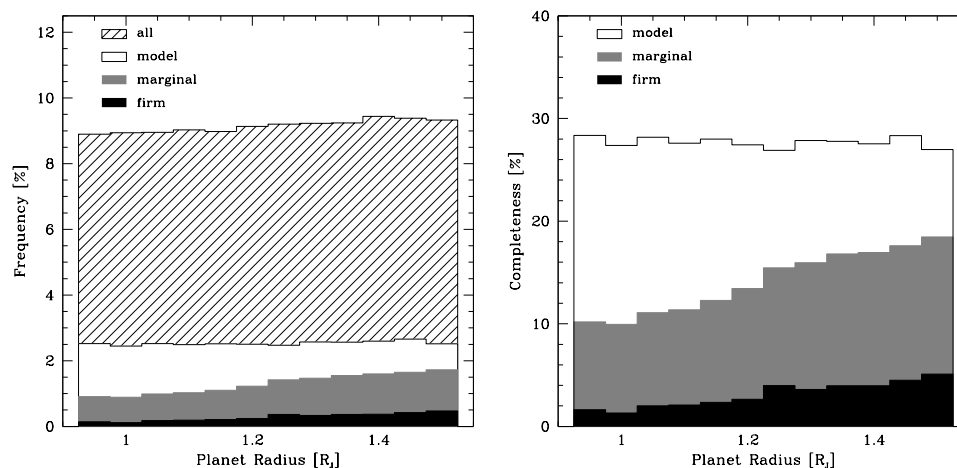


Fig. 5. Detection efficiency of planetary transits as a function of their radius, relative to planets with all inclinations (*left*) and all transiting planets (*right*).

### 5.1. Planet Frequency

The frequency of planets is known to increase with the host star's metallicity. From Figure 7 in Santos et al. (2004), the frequency of planets with metallicities below  $[\text{Fe}/\text{H}] = +0.1$  dex is  $\sim 2.5\%$ . The percentage of planets with periods below 10 days is 15%, as determined in Paper III. Combining these two numbers yields  $f_P = 0.375\%$ .

### 5.2. Detection Efficiency

In order to characterize our detection efficiency, we inserted model transits into the observed light curves, and tried to recover them using the BLS algorithm.

#### 5.2.1 Model Transit Light Curves

The transit light curves were generated using the approach described in Paper III. To obtain the radius and mass of the cluster stars, we used the  $Z=0.0198$ ,  $\tau = 7$  Gyr isochrone of Pietrinferni et al. (2004). A distance modulus  $(m - M)_R = 11.34$  mag was used to bring the observed  $R$ -band magnitudes to the absolute magnitude scale.

In addition to the period of the planet,  $P$ , the equations contain two other free parameters: the planet radius,  $R_P$  and the inclination of the orbit,  $i$ . A fourth parameter which affects the detectability of a planet is the epoch of the transits,  $T_0$ .

### 5.3. Test Procedure

We investigated the range of parameters specified in Table 1, where  $P$  is expressed in days,  $R_P$  in  $R_J$ ,  $T_0$  as a fraction of period. We examined the range of

periods from 1.05 to 9.85 days and planet radii from 0.95 to 1.5  $R_J$ , with a resolution of 0.2 days and 0.05  $R_J$ , respectively. For  $T_0$  we used an increment of 5% of the period, and a 0.025 increment in  $\cos i$ . The total number of combinations is 432000.

We followed the test procedure described in Paper III. The tests were run on the 2031 stars with at least 200 good epochs and light curve rms below 0.05 mag.

To assess the impact of the procedure to correct for offsets between the runs on our detection efficiency, we investigated three cases, where the correction was applied:

- A. after inserting transits,
- B. before inserting transits,
- C. was not applied at all.

Case (B) will give us the detection efficiency if our data did not need to be corrected, and case (C) if we did not apply the corrections. Case (A) will give us our actual detection efficiency, and its comparison with cases (B) and (C) will show how it is affected by the applied correction procedure.

#### 5.4. Detection Criteria

The same detection criteria as in Paper III were used. A transit was flagged as detected if:

1. The period recovered by BLS was within 2% of the input period  $P_{inp}$ ,  $2 P_{inp}$  or  $\frac{1}{2} P_{inp}$ ,
2. The BLS statistics were above the following thresholds:  $SDE > 5$ ,  $\alpha > 9$ .

These detections will be referred to hereafter as *firm*. Detections where only condition (1) was fulfilled will be called *marginal*.

#### 5.5. Detection Efficiency

The results of the tests are summarized in Table 2, which lists the test type (A-C), the number and percentage of transits with  $t_T \geq 0.5^h$  (out of the 432000 possible parameter combinations), and the numbers and percentages (relative to the total number of transits in column 2) of transits detected in the model light curves, and of marginal and firm detections in the combined light curves.

Figures 4 and 5 show the dependence of the detection efficiency on period and planet radius. The hatched, open, filled gray and filled black histograms denote distributions for all transiting planets, planets detected in the model light curves, and marginal and firm detections in the combined light curves, respectively. Left panels show the frequency of transits and transit detections relative to planets with all inclinations. Right panels show the detection completeness normalized to all transiting planets (plotted as hatched histograms in left panels).

The tests show that 9% of planets with periods 1-10 days will transit their parent stars. This frequency drops from  $\sim 20\%$  at  $P = 1^d$  to  $\sim 5\%$  at  $P = 10^d$ . The frequency of transits increases very weakly with planet radius.

The percentage of detections for the model light curves illustrates the limitation imposed on our detection efficiency by the temporal coverage alone. Due to incomplete time sampling, we are restricted to 28% of all planets with periods between 1 and 10 days. For periods below 3 days, our temporal coverage is sufficient to detect 57% of all transiting planets, and drops to 15% for periods 3 – 6 days and below 3% for periods 6 – 9 days. The detection completeness does not depend on the planet radius.

For cases A, B and C, we *marginally* detect 14%, 14% and 13% of all transiting planets, and *firmly* detect 3.1%, 3.3% and 2.7%, respectively. Transiting planets with firm detections constitute 68%, 69% and 68% of all stars with  $SDE > 5$  and  $\alpha > 9$ . Correcting the light curves after inserting transits (case A) produces almost the same number of detections, compared to the case where the correction was applied to the original light curves (case B). If the light curves were not corrected (case C), we would detect 82% of the transiting planets detected in case A.

The detection completeness for firm detections peaks at 15% for periods 1 –  $1.5^d$  and decreases with period more steeply than model detections. It strongly increases with increasing planet radius, from  $\sim 1.5\%$  at  $1 R_J$  to 5% at  $1.5 R_J$ .

The efficiency of *firm* transiting planet detections, relative to planets with all orbital inclinations,  $D$ , is  $1232/432000 = 0.29\%$ .

### 5.6. Number of Transiting Planets Expected

In §§ 5.1-5.2 we determined the planet frequency  $f_P$  to be 0.375%, the number of stars as 2031 and our detection efficiency  $D$  as 0.29%. We should thus expect 0.02 transiting planets among the cluster and field stars.

### 5.7. Discussion

Figure 4 demonstrates that our temporal coverage already places significant limits on our detection efficiency, restricting us to less than one third of all transiting systems with periods 1-10 days.

After the first observing run for this cluster we realized that this is not an optimal target for a transiting planet search, due to its low stellar density. We therefore chose to concentrate on NGC 2158 and to observe NGC 188 during the time of the night when the former cluster was unobservable, hence the limited temporal coverage.

## 6. Variable Stars

Table 3 lists the parameters of the previously known and newly discovered variable stars in NGC 188. It includes a membership probability estimate from Platais et al. (2003). The light curves of the variables are shown in Figures 6, 7 and 8.<sup>3</sup>

---

<sup>3</sup>The *VR* band photometry and finding charts for all variables are available from the authors from the PISCES website: <http://users.camk.edu.pl/mochejsk/PISCES/>.

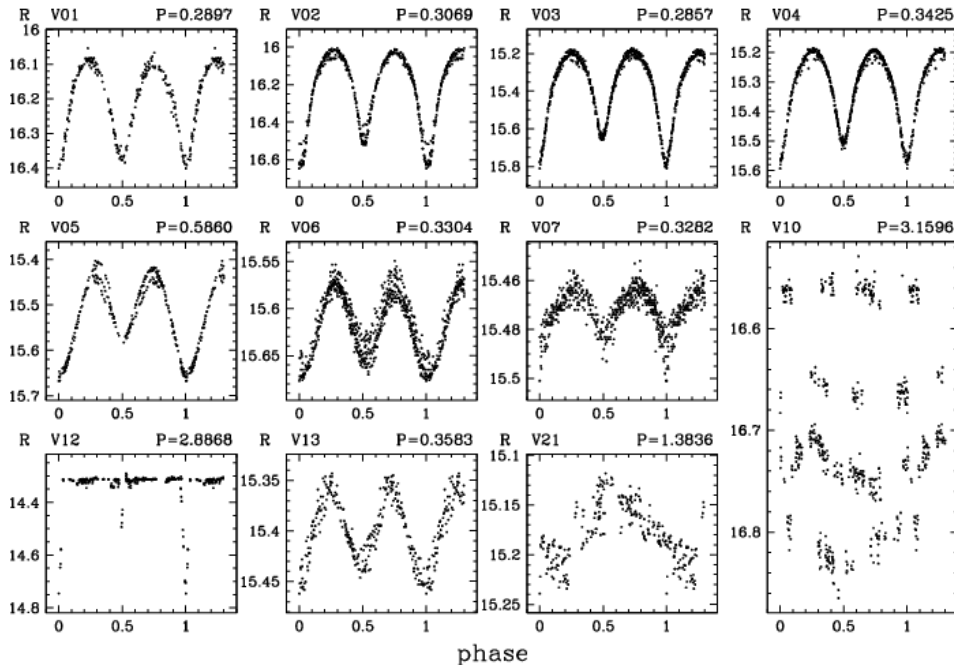


Fig. 6. *R*-band light curves of 11 previously known periodic variables. Data points from the first observing season are denoted by gray symbols and from the second season by black symbols. For variable V10 data from the four observing runs are plotted separately, with offsets of +0.3, +0.2, +0.1 and 0 mag, respectively.

They are also plotted on the CMD in Fig. 2.

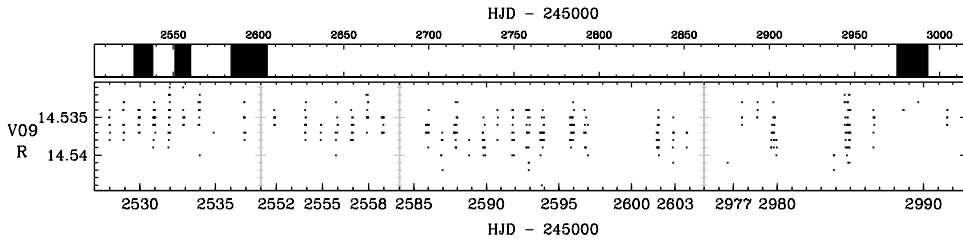


Fig. 7. *R*-band light curve of the previously known non-periodic variable V9. The top window illustrates the distribution in time of the four sub-windows plotted for the variable.

### 6.1. Previously Known Variables

NGC 188 has been the subject of several variability searches. Hoffmeister (1964) reported the first four variable stars in this cluster: EP, EQ, ER and ES Cephei (often referred to as V1-V4). Kaluzny & Shara (1987) identified six new variables, V5-V10, Kaluzny (1990) one, V11, Zhang et al. (2002) eight, V12-V19, and Zhang et al. (2004) another eight, bringing the total of known variables in this cluster to 27.

We identified variables V1-V7, V9, V10, V12, V13, V20 and V21 in our data.

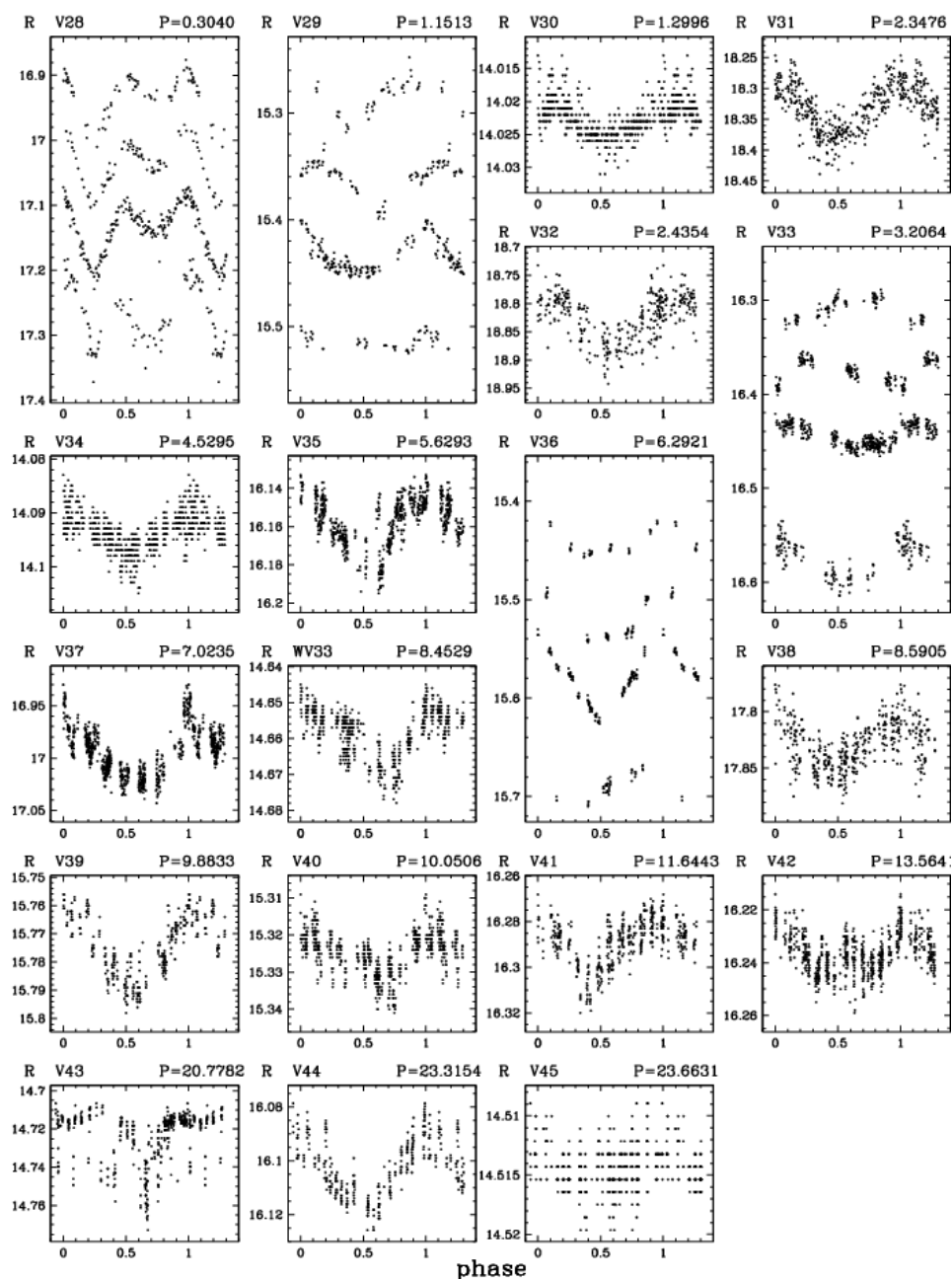


Fig. 8. *R*-band light curves of the previously known variable WV33 and 18 new variables V28-V45. Data points from the first observing season are denoted by gray symbols and from the second season by black symbols. For variables V28, V29, V33 and V36 data from the four observing runs are plotted separately, offset by 0.1, 0.08, 0.08 and 0.08 mag, respectively, between the runs, relative to the last season data (black points).

V8 and V11 were saturated on our images. The remaining 12 variables were outside our field of view.

Another study was performed by Kafka & Honeycutt (2003), who reported 51 variable stars, numbered WV1 through WV51. They identified their variables WV1, WV14 and WV11 with the previously known variables V1, V2 and V3. We identified 32 of their newly discovered variables in our fields: WV2-WV10, WV12, WV13, WV16-WV18, WV20-WV25, WV29, WV32-WV35, WV38, WV39, WV44-WV46, WV48, WV50. Two other variables, WV40 and WV41, were within our fields of view but we did not have photometry for them. We have examined their light curves and 31 of them did not display any kind of variability in our data. One variable, WV33, was found to vary with a period 5.5 times longer than the one reported by the authors. We also note that the coordinates for variables WV27, WV41 and WV44 disagree with their positions on the finder charts and that variable WV47 does not have any coordinates listed and it is not present on the finder charts.

Remarks on particular variables:

V1-V7: These variables are W UMa type contact binaries. We confirm their periods reported in the literature. We observe some variability in the shape of the light curves, especially for V5 and V6. V1, V2, V4 and V5 have high cluster membership probabilities ( $MP > 82\%$ ), V6 may be a cluster member ( $MP = 71\%$ ) and V3 and V7 are probably non-members ( $MP = 0\%$  and  $12\%$ , respectively). All of these stars, regardless of cluster membership, appear to be located on the cluster main sequence (MS) or above it, on the binary sequence.

V9: This variable shows very weak variability in our data. It is a cluster member ( $MP = 97\%$ ), located on the subgiant branch.

V10: This is a cluster member with probability 94%, located on the binary sequence. The phase, amplitude and the magnitude zero point of V10 are seen to vary between the observing runs. Kaluzny (1990) and Zhang et al. (2004) noted that in their data this star exhibited weak or no variability. This confirms that the variability amplitude of this star does indeed change with time. Kafka & Honeycutt (2003) determined a period of 3.1 days for this star, based on data from Kaluzny & Shara (1987), and we have found a similar period of 3.15 days in our observations. This is most likely a BY Dra type variable, where the variability is due to large spots on the star's surface rotating in and out of view.

V12: This is a detached eclipsing binary in the cluster ( $MP = 97\%$ ), located above the MSTO – a blue straggler. We have observed two eclipses and derive a period of 2.89 days, similar to the period of 2.81 days suggested by Zhang et al. (2004).

V13: This is a W UMa contact binary, a cluster member ( $MP = 98\%$ ), located above the MS. We derive a slightly longer period than Zhang et al. (2002; 2004).

V20: This star does not display variability in our data.

V21: This is a cluster member ( $MP = 92\%$ ), located on the MS. Our data do not confirm the period of 1.17 days found by Zhang et al. (2004). We find a period of 1.38 days, assuming that this is a BY Dra type variable. A period of 2.77 days

would be required to make this a W UMa system, as suggested by Zhang et al. (2004) – a rather unlikely scenario. A change in the variability amplitude is seen for this star.

WV33: This star is most likely not associated with the cluster ( $MP = 0\%$ ). It seems to be a BY Dra type variable with a period of 8.5 days. Our data exclude the period of 1.54 days suggested by Kafka & Honeycutt (2003).

### 6.2. *New Variables*

We searched for new variables by running BLS and Tatry (Schwarzenberg-Czerny & Beaulieu 2006) on the light curves of 6845 stars in fields A and B in the period ranges of 0.1-10 days and 0.1-100 days, respectively. We have discovered 18 new variables: 1, 3, 10 and 1 in field A chips 1-4 and 1 and 2 in field B chips 2 and 3. We have recovered 8 of the new 10 variables from chip A3 on chip B1. The remaining two variables were outside of the field of view. Of these new variables one is an eclipsing binary and 17 are other periodic variables.

V28 is a contact eclipsing binary and it displays long-term changes in the shape of the light curve. On the CMD it is located just above the MS. It may be a member of the cluster ( $MP = 59\%$ ).

The remaining 17 periodic variables display roughly sinusoidal light variations with periods ranging from 1.3 to 24 days. Most of them display BY Dra type of variability. V29, V33, V36 and V43, in addition to periodic variability, show a change in the variation amplitude, phase and magnitude zeropoint between the observing runs, which is most likely caused by the evolution of the spots on their surface.

Variables V29, V33-V35, V37, V39-V42 and V45 are likely cluster members, with  $MP$  ranging from 91% to 98%. V29, V39, V41 and V42 are located on the cluster MS. V33, V35, V37, V40 are located above the MS, on the cluster binary sequence, V45 is located on the subgiant branch and V34 is a blue straggler. For V31 and V32, the faintest variables in our sample, the membership probability estimates are inconclusive (53% and 46%, respectively). They are located near the cluster MS. V30, V36, V38, V43 and V44 are most likely not members of the cluster ( $MP = 0\%$ ).

## 7. Conclusions

In this paper we have performed a search for transiting planets in the old cluster NGC 188. The cluster was monitored for over 87 hours during 45 nights. Assuming a planet frequency from radial velocity surveys, we estimate that we should have detected 0.02 transiting planets with periods between 1 and 10 days, with our photometric precision and temporal coverage.

We have discovered 18 new variable stars in the old open cluster NGC 188: one eclipsing binary and 17 other periodic variables. Together with 28 previously

identified variables, this brings the total number of known variables in this cluster to 46. We have also presented high photometric precision light curves, spanning almost 15 months, for all previously known variables within our field of view.

**Acknowledgements.** We would like to thank the FLWO 1.2 m Time Allocation Committee for the generous amount of time we were allocated to this project.

Support for BJM was provided by the Polish KBN grant P03D012.30.

This publication makes use of data products from: the Two Micron All Sky Survey, which is a joint project of the University of Massachusetts and the Infrared Processing and Analysis Center/California Institute of Technology, funded by the National Aeronautics and Space Administration and the National Science Foundation; the Digital Sky Survey, produced at the Space Telescope Science Institute under U.S. Government grant NAG W-2166; the SIMBAD database, operated at CDS, Strasbourg, France and the WEBDA open cluster database maintained by J. C. Mermilliod (<http://obswww.unige.ch/webda/>).

Table 1

Parameter Range

Parameter	min	max	step	$n_{steps}$
P (days)	1.05	9.85	0.200	45
$R_P$ ( $R_J$ )	0.95	1.50	0.050	12
$T_0$	0.00	0.95	0.050	20
$\cos i$	0.0125	0.9875	0.025	40

Table 2

Artificial transit test statistics

test type	all transits		model		marginal		firm	
	N	%	N	%	N	%	N	%
1	39511	9.1	10940	27.7	5603	14.2	1232	3.1
2	39513	9.1	10939	27.7	5723	14.5	1300	3.3
3	39511	9.1	10940	27.7	5124	13.0	1060	2.7

## REFERENCES

- Alard, C. 2000, *Astronomy & Astrophysics Supplement*, **144**, 363.  
 Alard, C., Lupton, R. 1998, *Astrophysical Journal*, **503**, 325.

Table 3  
Variable stars in NGC 188

ID	$\alpha_{2000}$ [h]	$\delta_{2000}$ [°]	P [d]	$R$	$V$	$A_R$	$A_V$	Type	MP
V03	00 50 27.69	85 15 08.42	0.2857	15.188	15.727	0.608	0.557	E	0
V01	00 46 54.02	85 21 43.58	0.2897	16.096	16.617	0.290	0.276	E	98
V28	00 52 08.82	85 19 05.97	0.3040	17.190	17.862	0.145	0.126	E	59
V02	00 47 33.37	85 16 24.14	0.3069	16.025	16.591	0.604	0.562	E	82
V07	00 46 14.30	85 13 59.28	0.3282	15.460	15.872	0.036	0.043	E	12
V06	00 47 16.44	85 15 35.31	0.3304	15.565	16.045	0.109	0.095	E	71
V04	00 50 50.01	85 16 11.66	0.3425	15.193	15.703	0.378	0.360	E	96
V13	00 51 14.99	85 24 51.17	0.3583	15.355	15.791	0.100	0.088	E	98
V05	00 48 22.53	85 15 54.72	0.5860	15.426	16.034	0.232	0.220	E	95
V29	00 52 45.98	85 12 14.47	1.1513	15.519	15.956	0.026	0.026	P	98
V30	00 46 53.98	85 14 37.03	1.2996	14.023	14.319	0.005	0.003	P	0
V21	00 50 02.82	85 21 22.91	1.3836	15.173	15.577	0.067	0.069	P	92
V31	00 49 25.38	85 01 18.10	2.3476	18.335	19.182	0.090	0.119	P	53
V32	00 54 20.04	85 24 01.20	2.4354	18.836	19.764	0.090	0.124	P	46
V12	00 52 37.71	85 10 34.61	2.8868	14.308	14.712	0.334	0.281	E	97
V10	00 50 44.62	85 11 38.93	3.1596	16.840	17.471	0.033	0.028	P	94
V33	00 47 04.29	85 15 01.54	3.2064	16.540	17.163	0.025	0.027	P	93
V34	00 47 11.82	85 13 31.46	4.5295	14.094	14.454	0.007	0.007	P	98
V35	00 45 18.64	85 18 36.90	5.6293	16.161	16.692	0.039	0.040	P	97
V36	00 55 43.58	85 24 00.85	6.2921	15.669	16.158	0.055	0.061	P	0
V37	00 44 14.11	85 16 33.89	7.0235	16.999	17.714	0.057	0.052	P	91
WV33	00 51 15.85	85 09 47.86	8.4529	14.660	15.229	0.018	0.021	P	0
V38	00 44 30.63	85 01 29.68	8.5905	17.830	18.595	0.038	0.090	P	0
V39	00 39 05.98	85 18 39.32	9.8833	15.776	16.217	0.027	0.025	P	91
V40	00 44 52.20	85 15 54.34	10.0506	15.326	15.776	0.013	0.016	P	98
V41	00 49 36.46	85 06 26.08	11.6443	16.290	16.769	0.025	0.031	P	96
V42	00 48 54.98	85 17 12.61	13.5641	16.237	16.712	0.017	0.016	P	91
V43	00 36 39.97	85 03 18.20	20.7782	14.724	15.270	0.025	0.012	P	0
V44	00 48 25.86	85 12 23.35	23.3154	16.103	16.965	0.026	0.041	P	0
V45	00 44 40.60	85 15 21.22	23.6631	14.514	14.970	0.002	0.004	P	98
V09	00 44 52.25	85 10 25.01	...	14.536	15.095	0.011	0.016	L	97

Cluster membership probabilities  $MP$  taken from Platais et al. (2003).

Cutri, R. M., et al. 2003, *The 2MASS All-Sky Catalog of Point Sources (Pasadena: IPAC)*.

Hoffmeister, C. 1964, *Informational Bulletin on Variable Stars*, **67**, 1.

Kafka, S., & Honeycutt, R. K. 2005, *Astronomical Journal*, **130**, 742.

Kaluzny, J. 1990, *Acta Astronomica*, **40**, 61.

Kaluzny, J., & Shara, M. M. 1987, *Astrophysical Journal*, **314**, 585.

Kovács, G., Zucker, S., & Mazeh, T. 2002, *Astronomy & Astrophysics*, **391**, 369.

Mochejska, B. J., Stanek, K. Z., Sasselov, D. D., & Szentgyorgyi, A. H. 2002, *Astronomical Journal*, **123**, 3460 (Paper I).

Mochejska, B. J., Stanek, K. Z., Sasselov, D. D., Szentgyorgyi, A. H., Westover, M., & Winn, J. N. 2004, *Astronomical Journal*, **128**, 312 (Paper II).

Mochejska, B. J., et al. 2005, *Astronomical Journal*, **129**, 2856 (Paper III).

- Mochejska, B. J., et al. 2006, *Astronomical Journal*, **131**, 1090 (Paper IV).
- Pietrinferni, A., Cassisi, S., Salaris, M., & Castelli, F. 2004, *Astrophysical Journal*, **612**, 168.
- Platais, I., Kozhurina-Platais, V., Mathieu, R. D., Girard, T. M., & van Altena, W. F. 2003, *Astronomical Journal*, **126**, 2922.
- Santos, N. C., Israelian, G., & Mayor, M. 2004, *Astronomy & Astrophysics*, **415**, 1153.
- Sarajedini, A., von Hippel, T., Kozhurina-Platais, V., & Demarque, P. 1999, *Astronomical Journal*, **118**, 2894.
- Schwarzenberg-Czerny, A., & Beaulieu, J.-P. 2006, *MNRAS*, **365**, 165.
- Stetson, P. B. 1987, *PASP*, **99**, 191.
- Stetson, P. B., McClure, R. D., & Vandenberg, D. A. 2004, *PASP*, **116**, 1012.
- Tamuz, O., Mazeh, T., & Zucker, S. 2005, *MNRAS*, **356**, 1466.
- von Hippel, T., & Sarajedini, A. 1998, *Astronomical Journal*, **116**, 1789.
- Zhang, X. B., Deng, L., Zhou, X., & Xin, Y. 2004, *MNRAS*, **355**, 1369.
- Zhang, X. B., Deng, L., Tian, B., & Zhou, X. 2002, *Astronomical Journal*, **123**, 1548.